



NJC

**Highly phosphorescent green emitting iridium(III) complex
for application in OLEDs**

Journal:	<i>New Journal of Chemistry</i>
Manuscript ID:	NJ-ART-08-2014-001334.R2
Article Type:	Paper
Date Submitted by the Author:	01-Oct-2014
Complete List of Authors:	Jayabharathi, Jayaraman; Annamalai University, Chemistry Thanikachalam, Venugopal; Annamalai University, Chemistry Ramalingam, Sathishkumar; Annamalai University, Chemistry

SCHOLARONE™
Manuscripts

Highly phosphorescent green emitting iridium(III) complex for application in OLEDs

Jayaraman Jayabharathi*, Venugopal Thanikachalam, Ramalingam Sathishkumar

Department of Chemistry, Annamalai University, Annamalainagar 608 002, Tamilnadu, India.

*Address for correspondence

Dr. J. Jayabharathi

Professor of Chemistry

Department of Chemistry

Annamalai University

Annamalainagar 608 002

Tamilnadu, India.

Tel: +91 9443940735

E-mail: jtchalam2005@yahoo.co.in

Highly phosphorescent green emitting iridium(III) complex for application in OLEDs

Jayaraman Jayabharathi*, Venugopal Thanikachalam, Ramalingam Sathishkumar

Department of Chemistry, Annamalai University, Annamalainagar 608 002, Tamilnadu, India.

Abstract

Phenanthrimidazole based ligands with various substitution patterns have been used as the main ligand for heteroleptic bis cyclometalated iridium(III) complexes. Two series of complexes have been prepared by changing the ancillary ligand and their electroluminescent properties were studied. The strongly allowed phosphorescence in these complexes is the result of significant spin-orbit coupling of the iridium center. The absorption at longer wavelength have been assigned to $^1\text{MLCT} \leftarrow \text{S}_0$ and $^3\text{MLCT} \leftarrow \text{S}_0$ transitions of iridium complexes and the phosphorescence emission maxima range from 558 to 574 nm. The OLEDs with these picolate complexes exhibit appreciable external quantum efficiencies ranging from 6.5 to 15.6 %. Devices based with $\text{Ir}(\text{tmpmp})_2(\text{pic})$ and $\text{Ir}(\text{tmpdp})_2(\text{pic})$ show better performance in terms of brightness of 110421 cd/m^2 and 124568 cd/m^2 at 18 V, respectively. Device with $\text{Ir}(\text{tmpdp})_2(\text{pic})$ shows a high power efficiency of 25.6 lm/w at 7.0 V and current efficiency of 47.5 cd/A at 8.0 V. Introduction of dimethylamino group in 2-picolinate complexes, $\text{Ir}(\text{tmpmp})_2(\text{Npic})$ ($\eta_c = 44.6$, 8 V; $\eta_p = 26.0$, 7 V) and $\text{Ir}(\text{mpdp})_2(\text{Npic})$ ($\eta_c = 49.9$, 8 V; $\eta_p = 27.2$, 7 V) resulting in a highly phosphorescent green emitter with high electroluminescence efficiency.

Keywords: OLED; Electroluminescence; Green emitter; Iridium complex; Picolate.

1. Introduction

Electroluminescent heavy metal materials, namely iridium, platinum, ruthenium, and osmium complexes, have attracted considerable attention due to their potential applications in full color flat panel displays and solid-state lighting [1-6]. Among phosphorescent emitters, the best performing phosphorescent materials were those based on iridium(III) complexes because of the relatively short triplet lifetime and potential high device efficiency. Iridium(III)-based phosphorescent cyclometalated complexes are used as efficient dopants for applications in phosphorescent organic light-emitting diodes (PhOLEDs) [7-12], light-emitting electrochemical cells [13-16] and chemosensors [17,18]. The efficiency, brightness and emission wavelength of iridium(III) complexes depend strongly on the structure of the cyclometalated ligand. The emission wavelength of the iridium(III) complexes can normally be tuned by changing the electronic nature and position of the substituents on the ligands [19].

There is a crucial issue of phase separation between iridium(III) complexes and host materials that influence the doped device performance. This is overcome by increasing the bulkiness of the iridium(III) complexes which improve the dispersibility and thus high efficiency emission. A series of high efficiency iridium(III) complexes have been reported by introducing bulky cyclometalated ligands to effectively suppress the aggregation effect and improved the dispersibility [20-25]. Introduction of π -conjugated fluorenyl substituted triarylamine on the cyclometalated ligand improved the performance of the devices and also enhanced the solubility of the materials [21-24]. The dispersibility of iridium(III) complexes are also enhanced by modifying the ancillary ligand [26-30]. Phenylpyrazole based iridium(III) complexes, $\text{Ir}(\text{ppz})_3$ shows deep blue emission at 77 K in CH_2Cl_2 but quite poor emission at room temperature [31,32]. Their picolate complex, $\text{Ir}(\text{ppz})_2(\text{pic})$ shows relatively stronger green emission (526 nm) at room temperature and the emission color

changed from blue (422 nm) to orange red (587 nm) at low temperature (77 K) [33]. Continuing our interest to develop efficient green phosphors for application in OLEDs, herein we report a synthesis, characterization and electroluminescence of green emitting Ir(III) complexes containing bulky phenanthrimidazole ligands with picolinic acid (**1 - 4**) and 4-N,N-dimethylaminopicolinic acid (**5, 6**) as ancillary ligands. The emission properties of the synthesised iridium(III) complexes were studied and the device performance was examined for applications to OLEDs. Introduction of dimethylamino group in 2-picolinate resulting in a highly phosphorescent green emitter with high electroluminescence efficiency.

2. Experimental

2.1. Optical measurements and compositions analysis

The ^1H and ^{13}C NMR spectra at 400 and 100 MHz, respectively were obtained at room temperature using a Bruker 400 MHz NMR spectrometer (Bruker biospin, California, USA). The mass spectra of the samples were obtained using a Thermo Fischer LC-Mass spectrometer in fast atom bombardment (FAB) mode. The ultraviolet-visible (UV-vis) spectra of the phosphorescent iridium complexes were measured in an UV-vis spectrophotometer (Perkin Elmer Lambda 35) and corrected for background absorption due to solvent. Photoluminescence (PL) spectra were recorded on a fluorescence spectrometer (Perkin Elmer LS55). The PL quantum yields were measured by comparing phosphorescence intensities (integrated areas) of a standard sample (Coumarin 46) and the unknown sample using the formula, $\Phi_{\text{unk}} = \Phi_{\text{std}} \left(\frac{I_{\text{unk}}}{I_{\text{std}}} \right) \left(\frac{A_{\text{std}}}{A_{\text{unk}}} \right) \left(\frac{\eta_{\text{unk}}}{\eta_{\text{std}}} \right)^2$ where, Φ_{unk} is the phosphorescence quantum yield of the sample, Φ_{std} is the quantum yield of the standard; I_{unk} and I_{std} are the integrated emission intensities of the sample and the standard, respectively. A_{unk} and A_{std} are the absorbances of the sample and the standard at the excitation

wavelength, respectively. η_{unk} and η_{std} are the refractive indexes of the sample and standard solutions, respectively [34-36].

Cyclic voltammetry (CV) analysis were performed by using CHI 630A potentiostat electrochemical analyzer. Measurements of oxidation and reduction were undertaken using 0.1 mol/L tetra(n-butyl)ammoniumhexafluorophosphate as the supporting electrolyte, at scan rate of 0.1Vs^{-1} . The potentials were measured against an Ag/Ag^+ (0.01 mol/L AgNO_3) reference electrode using ferrocene/ferrocenium ($\text{CP}_2\text{Fe}/\text{CP}_2\text{Fe}^+$) as the internal standard. The onset potentials were determined from the intersection of two tangents drawn at the rising current and background current of the cyclic voltammogram. The lifetime was measured with a nanosecond time correlated single photon counting (TCSPC) spectrometer Horiba Fluorocube-01-NL lifetime system with Nano LED (pulsed diode excitation source) as the excitation source and TBX-PS as detector. DFT calculations were carried out in gas phase. All calculations were performed using density functional theory (DFT) as implemented with Gaussian-03 software package using the Becke3-Lee-Yang-Parr (B3LYP) functional [37] supplemented with LanL2DZ basis set [38] and LANL2DZ pseudopotentials were used for iridium metal and 6-31G* for carbon, hydrogen, oxygen, nitrogen and fluoro atoms

2.2. Device fabrication

The EL devices based on iridium(III) complexes were fabricated by vacuum deposition of the materials at 5×10^{-6} torr onto a clean glass precoated with a layer of indium tin oxide (ITO) with a sheet resistance of $20 \Omega/\text{square}$. Prior to use, the ITO surface was cleaned by sonication successively in a detergent solution, acetone, methanol and deionized water. Organic layers were deposited onto the substrate at a rate of 0.1 nm s^{-1} . The thickness of the organic materials and the cathode layers were controlled using a quartz crystal thickness monitor. A series of devices (I - VI) with configuration of ITO/NPB (30 nm)/iridium

complex: CBP (7%) (30 nm)/BCP (10 nm)/Alq₃ (40 nm)/Mg:Ag were fabricated. The device measurements of current, voltage and light intensity were made simultaneously using a Keithley 2400 sourcemeter. The EL spectra of the devices were carried out in an ambient atmosphere without further encapsulations.

2.3. General procedure for the synthesis of phenanthrimidazole ligands

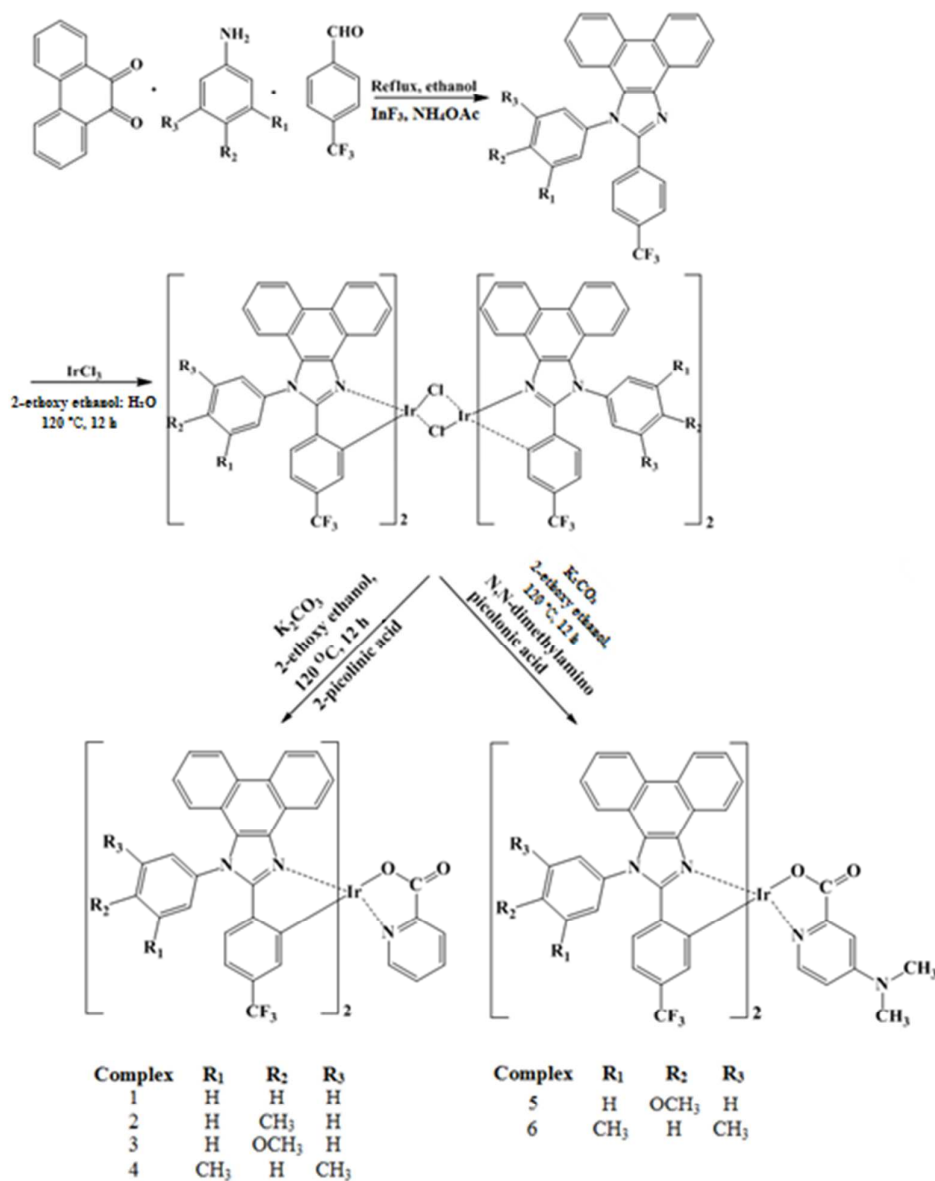
A mixture of phenanthrene-9, 10-dione (40 mmol), ammonium acetate (30 mmol), 4-trifluoromethylbenzaldehyde (30 mmol) and the corresponding arylamine (30 mmol) was refluxed in ethanol at 80°C in the presence of indium (III) fluoride (InF₃) as Lewis acid catalyst for 30 minutes. The reaction was monitored by thin layer chromatography and the crude phenanthrimidazoles were extracted with dichloromethane, purified by column chromatography using benzene-ethyl acetate (9:1) as the eluent. Yield: 95% (**1**), 96% (**2**), 94% (**3**) and 95% (**4**).

2.4. General procedure for the synthesis of chloro bridged dimers and iridium(III) complexes

IrCl₃ · xH₂O (1 mmol) was dissolved in a mixture of 2-ethoxyethanol/H₂O (3:1) by heating under nitrogen atmosphere around 90 °C for 30 min. The phenanthrimidazole ligand (2.3 mmol) in 2-ethoxyethanol was added and the solution was stirred at 120 °C for 12h. After cooling to room temperature, water was added and the precipitate was filtered, washed with water and ether and dried. The formed dimer was used without further purification.

The dimeric iridium(III) complex (0.54 mmol) was dissolved in 2-ethoxyethanol (2.5 ml). To this solution 2-picolinic acid (**1-4**) / 4-N,N-dimethylaminopicolinic acid (**5, 6**) (1.4 mmol) and K₂CO₃ (1.16 mmol) was added. The reaction mixture was refluxed under nitrogen atmosphere at 120 °C for 12h. After being cooled to room temperature, water was added; the precipitated green colour solid was collected by filtration and washed with

ethanol and hexane repeatedly. The residue was dissolved in dichloromethane and the solid was filtered and analysed [39] (Scheme-1).



Scheme 1. Synthetic route of iridium complexes

2.4.1. Iridium(III)bis(2-(4-trifluoromethylphenyl)-1-phenyl-1H-phenanthro[9,10-d]

imidazolato-*N,C*²) (picolinate), $[\text{Ir}(\text{tmpp})_2(\text{pic})]$, (**1**)

Yield: 79%. ¹H NMR (400 MHz, CDCl_3): δ 9.17 (d, 1H, $J = 8.0$ Hz), 8.62 (dd, 2H), 8.48 (dd, 1H), 8.38 (d, 1H, $J = 8.0$ Hz), 8.27 (d, 1H, $J = 8.0$ Hz), 8.09 (d, 1H, $J = 8.0$ Hz),

7.89-7.93 (m, 6H), 7.79 (t, 1H), 7.70 (d, 1H, $J = 8.0$ Hz), 7.64 (d, 1H, $J = 8.0$ Hz), 7.57 (t, 1H), 7.46-7.43 (m, 4H) 7.39 (t, 1H), 7.18-7.24 (m, 3H), 7.13 (d, 1H, $J = 8.0$ Hz), 7.07 (d, 1H, $J = 8.0$ Hz), 7.01 (d, 1H, $J = 8.0$ Hz), 6.72 (t, 1H), 6.63 (d, 1H, $J = 8.0$ Hz), 6.34-6.45 (m, 4H). ^{13}C NMR (100 MHz, CDCl_3): δ 27.36, 77.61, 106.31, 108.44, 108.63, 108.90, 119.97, 120.24, 121.67, 121.89, 122.24, 122.39, 122.89, 123.39, 123.56, 123.99, 124.14, 124.40, 125.29, 125.44, 125.77, 125.65, 125.72, 126.09, 126.19, 126.46, 126.68, 126.76, 126.78, 127.00, 127.40, 127.51, 128.47, 128.53, 128.74, 128.84, 129.23, 129.72, 129.94, 130.92, 131.09, 131.22, 131.46, 131.54, 131.70, 132.56, 133.33, 134.25, 137.49, 137.78, 146.24, 149.90, 150.66, 150.72, 152.75, 160.69, 160.80, 161.02, 162.12, 163.20, 163.54, 172.28, 192.45. Anal. calcd. for $\text{C}_{60}\text{H}_{36}\text{F}_2\text{IrN}_5\text{O}_2$: C, 66.16; H, 3.33; N, 6.43. Found: C, 66.67; H, 3.59; N, 6.54. MS: m/z 1089.73 [M^+].

2.4.2. Iridium(III)bis(2-(4-trifluoromethylphenyl)-1-p-tolyl-1H-phenanthro[9,10-d]

imidazolato-N,C²) (picolate), [Ir(tmptp)₂(pic)], (2)

Yield: 90%. ^1H NMR (400 MHz, CDCl_3): δ 9.17 (d, 1H, $J = 8.0$ Hz), 8.61 (dd, 2H), 8.47 (dd, 1H), 8.24 (dd, 2H), 8.08 (d, 1H, $J = 8.0$ Hz), 7.43-7.73 (m, 14H), 7.36 (t, 1H), 7.18-7.24 (m, 3H), 7.14 (d, 1H, $J = 7.6$ Hz), 7.00 (d, 1H, $J = 8.0$ Hz), 6.70 (t, 1H), 6.63 (d, 1H, $J = 8.8$ Hz), 6.44-6.52 (m, 3H), 6.35 (t, 1H), 2.71 (s, 3H), 2.68 (s, 3H). ^{13}C NMR (100 MHz, DMSO): δ 21.74, 21.80, 108.22, 108.45, 108.62, 108.85, 120.31, 120.56, 121.75, 122.10, 122.49, 122.93, 122.99, 123.33, 123.50, 123.93, 124.09, 124.35, 125.21, 125.36, 125.50, 125.70, 125.79, 126.13, 126.22, 126.41, 126.73, 126.82, 126.96, 127.01, 127.36, 127.57, 128.15, 128.44, 128.70, 128.84, 129.19, 129.55, 129.67, 131.49, 131.80, 131.87, 132.12, 132.65, 133.25, 134.20, 135.05, 135.07, 137.44, 141.28, 141.78, 146.24, 149.92, 150.58, 150.65, 152.74, 160.66, 160.86, 162.17, 163.16, 163.52, 172.28. Anal. calcd. for $\text{C}_{62}\text{H}_{40}\text{F}_2\text{IrN}_5\text{O}_2$: C, 66.65; H, 3.61; N, 6.27. Found: C, 66.78; H, 3.68; N, 6.32. MS: m/z 1117.60 [M^+].

2.4.3. Iridium(III)bis(2-(4-trifluoromethylphenyl)-1-(4-methoxyphenyl)-1H-phenanthro

[9,10-d]imidazolato-*N,C*²')(picolinate), [Ir(tmpmp)₂(pic)], (3)

Yield: 86%. ¹H NMR (400 MHz, CDCl₃): δ 9.16 (d, 1H, *J* = 8.0 Hz), 8.63 (dd, 2H), 8.50 (dd, 1H), 8.27 (d, 2H, *J* = 7.2 Hz), 8.20 (d, 1H, *J* = 8.0 Hz), 8.07 (d, 1H, *J* = 8.0 Hz), 7.79 (d, 1H, *J* = 8.0 Hz), 7.22-7.63 (m, 18H), 6.98 (d, 1H, *J* = 7.6 Hz), 6.74 (t, 1H), 6.49-6.57 (m, 4H), 6.38 (t, 1H), 4.11 (s, 3H), 4.09 (s, 3H). ¹³C NMR (100 MHz, CDCl₃): δ 55.85, 55.94, 107.73, 107.86, 108.28, 108.50, 109.82, 115.79, 115.90, 116.17, 116.28, 116.59, 122.10, 122.94, 122.96, 123.54, 123.94, 124.11, 124.34, 125.20, 125.38, 125.50, 125.69, 126.70, 126.83, 126.93, 127.02, 127.35, 127.68, 128.23, 128.43, 128.72, 129.53, 129.69, 129.83, 130.06, 130.14, 130.24, 130.97, 137.44, 146.24, 150.02, 150.73, 152.87, 159.19, 161.07, 161.21, 161.44. Anal. calcd. for C₆₂H₄₀F₂IrN₅O₄: C, 64.80; H, 3.51; N, 6.09. Found: C, 64.77; H, 3.60; N, 6.15. MS: *m/z* 1149.53 [M⁺].

2.4.4. Iridium(III)bis(2-(4-trifluoromethylphenyl)-1-(3,5-dimethylphenyl)-1H-phenanthro

[9,10-d]imidazolato-*N,C*²')(picolinate), [Ir(tmpdp)₂(pic)], (4)

Yield: 91%. ¹H NMR (400 MHz, DMSO): δ 9.19 (d, 1H, *J* = 6.8 Hz), 8.56 (dd, 2H), 8.27 (dd, 1H), 7.92 (dd, 2H), 7.73 (d, 1H, *J* = 9.6 Hz), 7.48-7.69 (m, 14H), 7.40 (t, 1H), 7.25-7.28 (m, 6H), 7.23 (d, 1H, *J* = 8.0 Hz), 7.09 (d, 1H, *J* = 8.8 Hz), 6.72 (t, 1H), 6.64 (d, 1H, *J* = 8.4 Hz), 6.46-6.52 (m, 3H), 6.38 (t, 1H), 4.11 (s, 3H), 4.09 (s, 3H). ¹³C NMR (100 MHz, DMSO): δ 21.71, 21.76, 29.72, 29.87, 108.21, 108.44, 108.61, 108.85, 120.31, 120.56, 121.93, 122.01, 122.49, 122.92, 123.01, 123.33, 123.50, 123.92, 124.08, 124.34, 125.20, 125.35, 125.49, 125.69, 126.40, 126.73, 126.80, 126.90, 126.99, 127.36, 127.57, 128.14, 128.43, 128.70, 128.83, 129.18, 129.67, 131.47, 131.82, 131.86, 132.10, 133.25, 134.19, 135.05, 135.07, 137.42, 160.65, 160.87, 162.18, 163.19, 172.25. Anal. calcd. for C₆₄H₄₄F₂IrN₅O₂: C, 67.12; H, 3.87; N, 6.11. Found: C, 67.14; H, 3.84; N, 6.15. MS: *m/z* 1145.47 [M⁺].

2.4.5. Iridium(III)bis(2-(4-trifluoromethylphenyl)-1-(4-methoxyphenyl)-1H-phenanthro

[9,10-d]imidazolato-*N,C*²)(4-*N,N*-dimethylaminopicolinate) [Ir(tmpmp)₂(Npic)], (5)

Yield: 86%. ¹H NMR (400 MHz, DMSO): δ 9.11 (d, 1H, *J* = 8.0 Hz), 8.58 (dd, 2H), 8.45 (dd, 1H), 8.22 (d, 2H, *J* = 7.2 Hz), 8.15 (d, 1H, *J* = 8.0 Hz), 8.02 (d, 1H, *J* = 8.0 Hz), 7.74 (d, 1H, *J* = 8.0 Hz), 7.18-7.58 (m, 18H), 6.93 (d, 1H, *J* = 7.6 Hz), 6.70 (t, 1H), 6.46-6.53 (m, 4H), 6.34 (t, 1H), 4.8 (s, 3H), 4.03 (s, 3H), 3.08 (s, 6H). ¹³C NMR (100 MHz, DMSO): δ 39.6, 55.80, 55.89, 107.68, 107.81, 108.23, 108.45, 109.77, 115.74, 115.85, 116.12, 116.23, 116.54, 122.05, 122.89, 122.91, 123.50, 123.88, 124.07, 124.29, 125.15, 125.33, 125.45, 125.64, 126.65, 126.77, 126.88, 126.07, 127.30, 127.63, 128.17, 128.38, 128.67, 129.48, 129.64, 129.78, 129.00, 130.08, 130.18, 130.93, 137.39, 146.18, 149.93, 150.67, 152.82, 159.12, 161.05, 161.15, 161.38. Anal. calcd. for C₃₈H₃₀F₃IrN₄O₃: C, 54.34; H, 3.60; F, 6.79; N, 6.67. Found: C, 54.32; H, 3.58; F, 6.78; N, 6.65. MS: *m/z* 839.88 [M⁺].

2.4.6. 2-(4-trifluoromethylphenyl)-1-(3,5-dimethylphenyl)-1H-phenanthro[9,10-d]

imidazolato-*N,C*²)(4-*N,N*-dimethylaminopicolinate) [Ir(mpdp)₂(Npic)], (6)

Yield: 91%. ¹H NMR (400 MHz, DMSO): δ 9.14 (d, 1H, *J* = 6.8 Hz), 8.51 (dd, 2H), 8.22 (dd, 1H), 7.87 (dd, 2H), 7.67 (d, 1H, *J* = 9.6 Hz), 7.43-7.64 (m, 14H), 7.35 (t, 1H), 7.20-7.23 (m, 6H), 7.19 (d, 1H, *J* = 8.0 Hz), 7.03 (d, 1H, *J* = 8.8 Hz), 6.68 (t, 1H), 6.59 (d, 1H, *J* = 8.4 Hz), 6.41-6.48 (m, 3H), 6.33 (t, 1H), 4.08 (s, 3H), 4.03 (s, 3H), 3.04 (s, 6H). ¹³C NMR (100 MHz, DMSO): δ 21.67, 21.71, 29.67, 29.82, 39.40, 108.17, 108.39, 108.55, 108.80, 120.26, 120.51, 121.88, 121.94, 122.44, 122.87, 122.98, 123.27, 123.45, 123.87, 124.01, 124.29, 125.15, 125.30, 125.44, 125.64, 126.35, 126.68, 126.76, 126.84, 126.94, 127.31, 127.52, 128.08, 128.38, 128.66, 128.78, 129.11, 129.60, 131.42, 131.79, 131.81, 132.05, 133.21, 134.12, 135.00, 135.02, 137.38, 160.61, 160.82, 162.11, 163.13, 172.20. Anal. calcd. for C₃₉H₃₂F₃IrN₄O₂: C, 55.90; H, 3.85; F, 6.80; N, 6.69. Found: C, 55.88; H, 3.84; F, 6.77; N, 6.67. MS: *m/z* 837.91 [M⁺].

3. Results and discussion

3.1 Synthesis and Characterization of iridium(III) Complexes

The synthetic method used to prepare these complexes involves two steps. In the first step, $\text{IrCl}_3 \cdot 3\text{H}_2\text{O}$ was allowed to react with an excess of the cyclometalated phenanthrimidazole ligand to give a chloride-bridged dinuclear complex. The chloride-bridged dinuclear complexes can be readily converted to emissive, mononuclear complexes by replacing the two bridging chlorides with bidentate picolinic acid (**1** - **4**) and 4-N,N-dimethylaminopicolinic acid (**5**, **6**) as ancillary ligands. The yield of the reactions is 79-91%. All the mononuclear complex dopants are thermally stable up to 368-393°C and can be sublimed easily at reduced pressure. The synthesised complexes were characterised by ^1H and ^{13}C NMR, mass spectra (MS) and CHN analysis and analysed.

3.2. Photophysical studies

The absorption and emission spectra of iridium(III) complexes in dichloromethane at room temperature were shown in figure 1. The intense band around 297 nm in the ultraviolet part of the spectrum can be assigned to the allowed ligand centered ($\pi\text{-}\pi^*$) transitions [40]. The weak absorption bands in the range 379-434 nm have been assigned to MLCT transitions ($^1\text{MLCT} \leftarrow \text{S}_0$ and $^3\text{MLCT} \leftarrow \text{S}_0$) [41-45]. The intensity of $^3\text{MLCT} \leftarrow \text{S}_0$ are strongly close to the intensity of $^1\text{MLCT} \leftarrow \text{S}_0$ suggesting that $^3\text{MLCT} \leftarrow \text{S}_0$ is strongly allowed by S-T mixing due to spin orbit coupling. Strong spin orbit coupling makes these complexes as highly phosphorescent in nature [46,47].

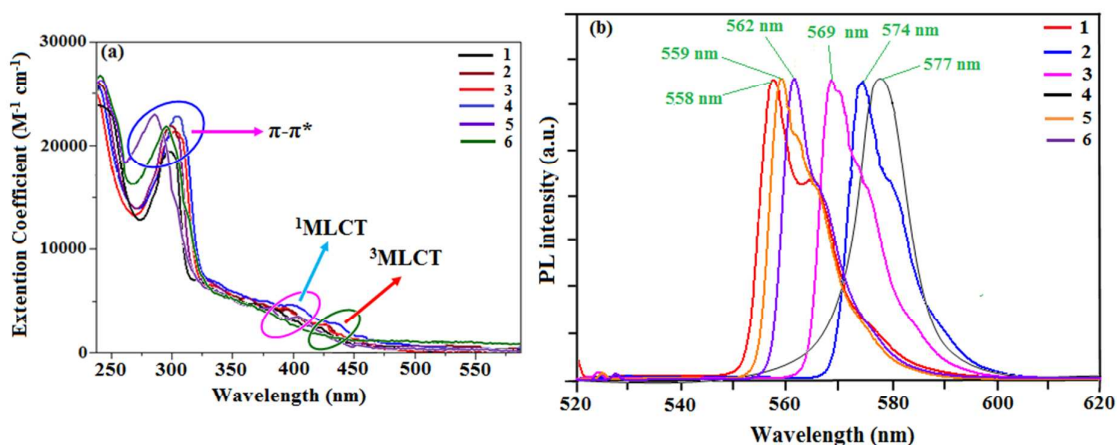


Figure 1. Absorption and emission spectra of the iridium complexes **1–6** in CH_2Cl_2

Emission from these mononuclear metal complexes reveal that the phosphorescence is attributed to a mixture of both metal-ligand charge-transfer $^3(\text{MLCT})$ and $^3(\pi-\pi^*)$ states. The wavefunction of the excited triplet state (Φ_T), is responsible for the phosphorescence i.e., $\Phi_T = a \Phi_T(\pi-\pi^*) + b \Phi_T(\text{MLCT})$, where ‘ a ’ and ‘ b ’ are the normalized co-efficient, $\Phi_T(\pi-\pi^*)$ and $\Phi_T(\text{MLCT})$ are the wavefunction of $^3(\pi-\pi^*)$ and $^3(\text{MLCT})$ excited states, respectively. For these iridium complexes, the wavefunction of the triplet state (Φ_T) is responsible for the phosphorescence and the equation implies that the excited triplet state of these iridium complexes are a mixture of $\Phi_T(\pi-\pi^*)$ and $\Phi_T(\text{MLCT})$. The triplet state is attributed to dominantly $^3\pi-\pi^*$ excited state when $a > b$ and dominantly $^3\text{MLCT}$ excited state when $b > a$ [48-50]. According to our previous studies [44,45], phosphorescence spectra from the ligand centered $^3\pi-\pi^*$ state display vibronic progressions and those from the $^3\text{MLCT}$ state are broad in shape. In the present study, complexes **1-3**, **5** and **6** display vibronic progressions having excited state with large contribution of $^3\pi-\pi^*$ whereas the emission spectrum of complex $\text{Ir}(\text{tmpdp})_2(\text{pic})$ **4** is broad in shape and has excited state with large contribution of $^3\text{MLCT}$. All these complexes show dominant emission at 558, 574, 569, 577, 559 and 562 nm and shoulder peak around 565 (**1**), 579 (**2**) and 574 nm (**3**) in dichloromethane, respectively (Table 1). Molecules having intramolecular donor-acceptor

(DA) systems exhibit bathochromic shift in electronic spectra. Phenanthrimidazole derivative has a DA character [51] resulting from the interaction between the electron rich phenanthrimidazole moiety and an electron deficient trifluoromethylphenyl group. The introduction of an electron releasing methyl and methoxy groups into the phenanthrimidazole moiety is considered to enhance the DA character of the ligand. The emission of their corresponding iridium(III) complexes **2-6** are red shifted [16 (**2**), 11 (**3**), 19 (**4**), 1 (**5**) and 4 nm (**6**)] when compared with complex Ir(tmpp)₂(pic) **1** and this may be due to the electronic effect and position of the substituents. The observed results indicate that the introduction of the methyl and methoxy groups into the phenanthrimidazole fragment enhance the DA character of the ligand in the iridium(III) complexes leading to red shift (Figure 1). There is significantly blue shift observed for complexes **5** and **6** on comparison with their analogues complexes **3** and **4**. This interesting behaviour may be due to the presence of donor N,N-dimethylamino group in the ancillary ligand of 2-picolinate.

The dominant and shoulder emissions from complexes **1-3** are explained as follows. The ground and excited states of organic light-emissive materials are composed of several separated vibrational states ($v = 0, 1, 2, \dots$) according to the Franck - Condon principle. The emissive spectra of iridium(III) complexes **1-3** consist of two kinds of peak, 558, 565 (sh) nm (**1**), 574, 579 (sh) nm (**2**) and 569, 574 (sh) nm (**3**) corresponding to the electronic transitions between the vibrational levels of the triplet state ($^3\text{MLCT}/^3\pi-\pi^*$) and ground state (S_0). The peak with dominant intensity stemmed from 0 to 0 electronic transition between $^3\text{MLCT}/^3\pi-\pi^*$ and S_0 and a shoulder with lower intensity derived from 0 to 1 electronic transition [52,53]. The representative Franck - Condon electronic transitions are shown in Figure 2.

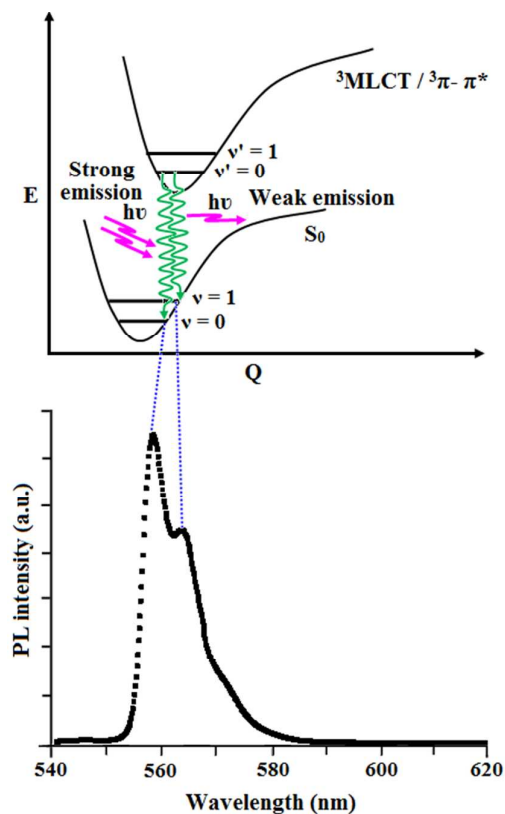


Figure 2. Representative Franck - Condon electronic transitions

The radiative and non-radiative decay of the excited state of iridium complexes have been obtained using the quantum yield (Φ) and lifetime (τ). The decay curve is shown in figure 3. The radiative lifetimes are in the microsecond range as expected for cyclometalated iridium(III) complexes. The formula employed to calculate the radiative (k_r) and non-radiative (k_{nr}) rate constants are, $\Phi = \Phi_{ISC} \{ k_r / (k_r + k_{nr}) \}$; $k_r = \Phi / \tau$; $k_{nr} = (1/\tau) - (\Phi/\tau)$; $\tau = (k_r + k_{nr})^{-1}$, where, Φ_{ISC} is the intersystem-crossing yield. For the iridium complexes, Φ_{ISC} is safely assumed to be 1.0 because of the strong spin-orbit interaction caused by heavy atom effect of iridium [54]. The decay parameter, radiative (k_r) and non-radiative (k_{nr}) rate constants are displayed in Table 1. Perusal of the radiative and non-radiative rate constants shows that the radiative emission is predominant over non-radiative transitions in these complexes [55-57].

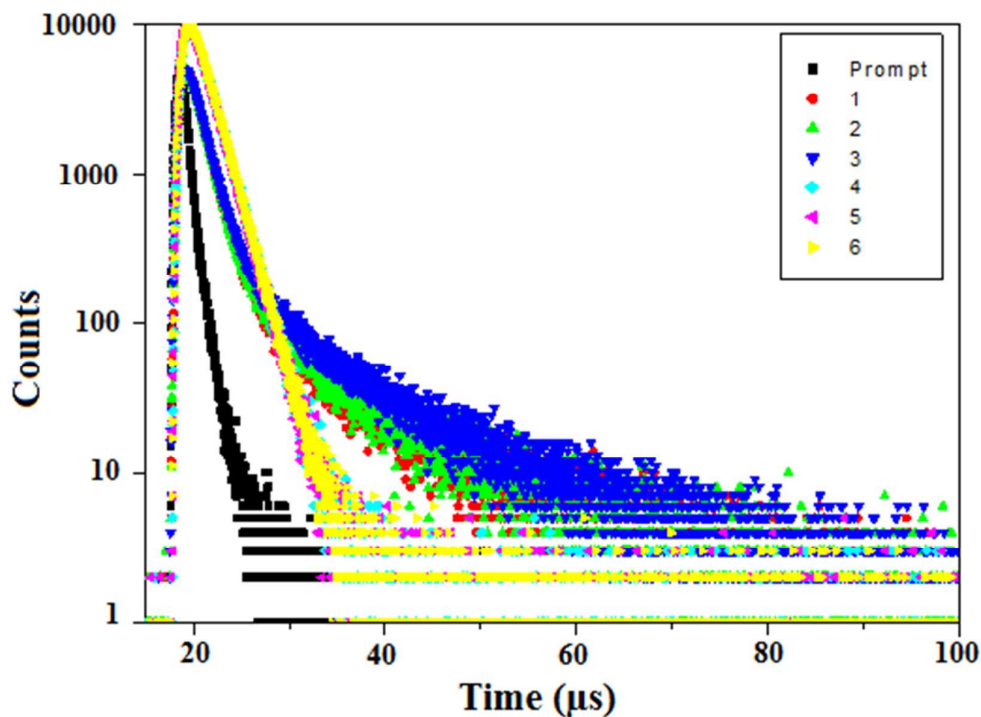


Figure 3. Lifetime spectra of the iridium complexes **1–6** in CH_2Cl_2

Experimentally observed result indicates that the radiative rate constant (k_r) of complexes $\text{Ir}(\text{tmtp})_2(\text{pic})$ **2** and $\text{Ir}(\text{tmpmp})_2(\text{pic})$ **3** increases with an increase of E_{emi} . According to the electronic transition theory, the k_r value is proportional to the square of the electric dipole transition moment (M_{T-S}). The first-order perturbation theory gives an approximate expression for M_{T-S} [58], $M_{T-S} = \sum \beta_n \langle {}^1\phi_n | M | {}^1\phi_0 \rangle$, where ${}^1\phi_n$ and ${}^1\phi_0$ are the wavefunctions of the S_n and S_0 states, respectively and M is the electric dipole vector. With the use of the spin-orbit coupling operator (H_{so}) and the wavefunction of the lowest excited triplet state (${}^3\phi_1$), β_n is formulated as, $\beta_n = \langle {}^1\phi_1 | H_{\text{SO}} | {}^3\phi_1 \rangle / ({}^1E_n - {}^3E_1)$, where 1E_n and 3E_1 are the energies of S_n state and lowest excited triplet state, respectively. Here, we assume a three state model S_1 , T_1 and S_0 , now, the above equation becomes, $M_{T-S} = \{ \langle {}^1\phi_1 | H_{\text{SO}} | {}^3\phi_1 \rangle \langle {}^1\phi_1 | M | {}^1\phi_0 \rangle \} / ({}^1E_1 - {}^3E_1) = \alpha / ({}^1E_1 - {}^3E_1)$, when ($\alpha = \langle {}^1\phi_1 | H_{\text{SO}} | {}^3\phi_1 \rangle \langle {}^1\phi_1 | M | {}^1\phi_0 \rangle$) is constant, k_r increases with a decrease in the energy difference (${}^1E_1 - {}^3E_1$). In the present study, k_r increases (Figure S1) with an increase of E_{emi} for complexes $\text{Ir}(\text{tmtp})_2(\text{pic})$ **2** and $\text{Ir}(\text{tmpmp})_2(\text{pic})$ **3** which is

explained by assuming that the S_1 energy does not differ significantly and the energy difference (${}^1E_1 - {}^3E_1$) increases with decrease of E_{emi} . For complexes **2** and **3**, the $S_1 \leftarrow S_0$ absorption bands are located at 304 and 297 nm but phosphorescence $S_0 \leftarrow T_1$ exhibits large bathochromic shift ranging from 574 and 569 nm. This is evidence that the energy difference (${}^1E_1 - {}^3E_1$) increases with the decrease of E_{emi} and therefore, k_r increases with an increase of E_{emi} .

In order to investigate the highest occupied molecular orbital (HOMO) and the lowest unoccupied molecular orbital (LUMO) energy levels, cyclic voltammetric analyses was carried out (Figure 4a). The redox potentials of the cyclometalated iridium complexes were measured relative to an internal ferrocene reference ($\text{Cp}_2\text{Fe}/\text{Cp}_2\text{Fe}^+ = 0.45\text{V}$ versus SCE in CH_2Cl_2 solvent) [59-62]. The reduction occurs primarily on the more electron accepting heterocyclic portion of the cyclometalated phenanthrimidazole ligands whereas the oxidation largely involve in the iridium-phenyl centre. The calculated energies of HOMO and LUMO are given in Table 1. The HOMO energy levels were calculated using the equation, $E_{\text{HOMO}} (\text{eV}) = - (E_{\text{ox}}^{\text{onset}} - E_{\text{Fc}/\text{Fc}^+}^{\text{onset}}) - 4.80 \text{ eV}$, where $E_{\text{ox}}^{\text{onset}}$ and $E_{\text{Fc}/\text{Fc}^+}^{\text{onset}}$ are the onset oxidation potential of the iridium complexes and ferrocene, respectively. The LUMO energies are calculated based on the HOMO energies and the lowest energy absorption edges of the absorption spectra [60], $E_{\text{LUMO}} (\text{eV}) = E_{\text{HOMO}} - 1239/\lambda_{\text{onset}}$ [63]. The HOMO energy levels of the complexes **1-6** were calculated to be 5.60, 5.62, 5.61, 5.54, 5.52 and 5.45 eV, respectively [64]. From the energy gap it was concluded that all the reported dopants are green emitters (Figure 4b). The 3D orbitals of HOMO and LUMO of $\text{Ir}(\text{tmpp})_2$ (pic **1**) are shown in Figure 4c.

Table 1. Absorption (λ_{abs} , nm), emission (λ_{emi} , nm), fluorescence quantum yield (Φ), electrochemical behaviour life time (τ , μs) and emission kinetics of **1- 6**

Complex	λ_{abs}	λ_{emi}	Φ	E_{onset}	$E^{1/2}_{\text{oxi}}$ (V)	HOMO (eV)	LUMO (eV)	E_g (eV)	τ	k_r 10^8s^{-1}	k_{nr} 10^8s^{-1}
1	301, 379, 421	558	0.55	456	0.80	5.60	2.88	2.72	1.88	2.9	2.4
2	304, 394, 432	574	0.53	443	0.82	5.62	2.82	2.80	1.92	2.8	2.5
3	297, 387, 425	569	0.56	447	0.81	5.61	2.84	2.77	1.94	2.9	2.2
4	305, 399, 434	577	0.58	440	0.74	5.54	2.73	2.81	1.80	3.2	2.3
5	283, 371, 416	559	0.57	455	0.72	5.52	2.80	2.72	1.72	3.4	2.4
6	298, 382, 420	562	0.59	449	0.65	5.45	2.69	2.76	1.74	3.5	2.2

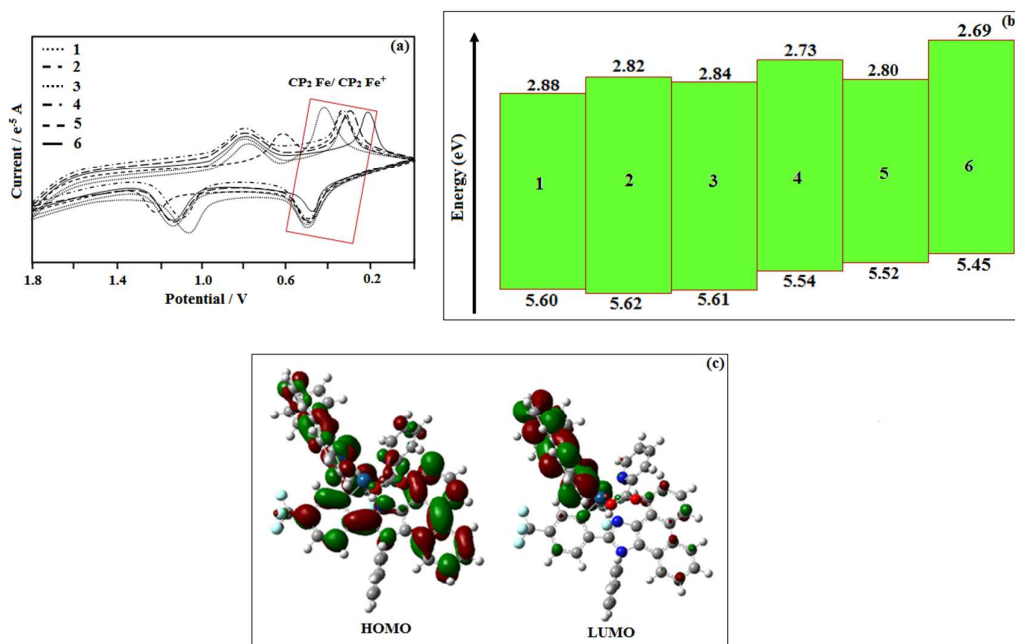


Figure 4. (a) Cyclic voltammogram curves of the iridium complexes **1–6**; (b) Schematic representation of HOMO – LUMO energies of **1–6**; (c) The HOMO-LUMO orbital picture of Ir(tmpp)₂(pic) **1**

3.2. Structure of Ir(tmpp)₂(pic) **1**

All the synthesized Ir(III) complexes are amorphous solid and single crystal X-ray analysis could not be made. Thus the optimization has been made using density functional theory, LANL2DZ pseudopotentials for iridium metal and 6-31G* for carbon, hydrogen, oxygen, nitrogen and fluoro atoms. The selected bond length and bond angle for Ir(tmpp)₂(pic) **1** are presented in Table 2. The x, y and z coordinates are displayed in Table S1. The optimized geometry of the complex shows that the complex exhibits an octahedral geometry around metal iridium and prefers *cis* –C,C and *trans*-N,N chelate disposition instead of *trans*- C,C and *trans*-N,N chelate. Electron rich phenyl rings normally exhibit very strong influence and *trans* effect. Therefore, the *trans*-C,C arrangement is expected to be thermodynamically higher in energy and kinetically more labile [62]. The Ir-C bonds of the complex i.e Ir-C_{av} is 2.038 Å, which is shorter than Ir-N bonds i.e., Ir-N_{av} is

2.060 Å. The Ir–O bond length [2.138 Å] is longer than the mean Ir–O bond length (2.088Å) reported [63] and these observations reflect the *trans* influence of the phenyl groups. This arrangement of the ligands is similar to that found in other mononuclear iridium(III) complexes that possess an Ir(ppy)₂ fragment [65-68] (Figure S2).

Table 2. Selected Bond lengths (Å) and Bond angle (°) of Ir(tmpp)₂(pic) **1**

Connectivity	Bond length	Connectivity	Bond angle
Ir(1)–C(2)	2.008	C(3)–Ir(1)–C(8)	87.41
Ir(1)–C(9)	2.021	C(7)–C(9)–F(85)	94.65
C(31)–N(2))	1.543	C(12)–C(16)–F(86)	166.90
C(7)–N(4)	1.538	N(37)–C(30)–N(39)	91.08
Ir(1)–C(24)	1.798	O(41)–C(38)–O(40)	89.73
Ir(1)–C(39)	2.002	C(44)–C(29)–N(39)	91.76

3.3. Thermal studies

The thermal properties of the iridium(III) complexes have been investigated by thermogravimetric analyses (TGA) under nitrogen atmosphere. The iridium complexes exhibits high thermal stability. Ir(tmpp)₂(pic) decomposition begins at about 379 °C and proceeds in three stages. Ir(tmptp)₂(pic) decomposition begins at about 368 °C and proceeds in four stages. (Ir(tmpmp)₂(pic) decomposition begins at about 383 °C and proceeds in three stages. Ir(tmpdp)₂(pic) decomposition begins at about 374 °C. Decomposition of complexes **5** and **6** begins at 390 °C and 395 °C, respectively, as shown in Figure 5a. The thermal stability of the complexes has also been explained by differential scanning calorimetry (DSC). Figure 5b indicates that the iridium complexes undergo a glass transition around 93°C, followed by crystallization around 112 °C and crystalline melting at 380, 382, 369, 373, 385 and 388 °C for **1-6**, respectively.

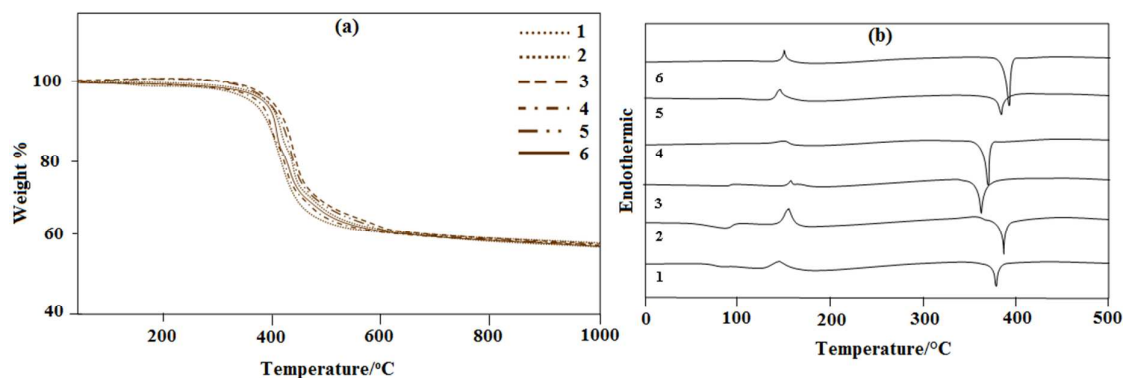


Figure 5. (a) TG-DTA curves of the iridium complexes **1–6**; (b) DSC curves of the iridium complexes **1–6**

3.4. Electroluminescent properties

OLED devices using the synthesised iridium(III) complexes as dopants have been fabricated with multi-layer configuration of ITO/NPB (30 nm)/iridium complex: CBP (7%) (30 nm)/BCP (10 nm)/Alq₃ (40 nm)/Mg:Ag where, ITO was used as the anode, NPB (4,4'-bis[N-(1-naphthyl)-N-phenylamino]biphenyl) was used as the hole-transporting material, CBP (4,4'-N,N'-dicarbazole biphenyl) as the host, the iridium complexes as the dopant, BCP (2,9-dimethyl-4,7-diphenyl-1,10-phenanthroline) as the hole blocker, Alq₃ (tris(8-hydroxyquinolino) aluminium) as the electron transporter and Mg:Ag as the cathode (Figure 6a). The performance of these devices is listed in Table 3. The devices emit strong green light with an emission maximum at 563, 578, 572, 584, 561 and 564 nm, respectively (Figure 6b).

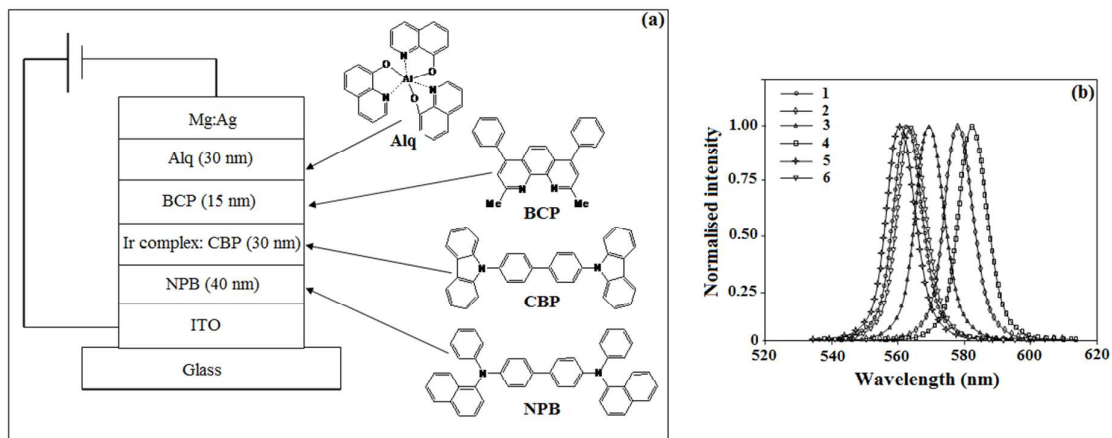


Figure 6. (a) General structure of device; (b) Electroluminescence spectra of 1–6 in CH_2Cl_2

Figures 7a and 7b show the brightness–voltage and the external quantum yield–current density characteristics of the devices, respectively. All devices show quite appreciable efficiencies and brightness. Of the six devices, device II shows poor efficiency followed by device I. The external quantum efficiency of device II is low; even at driven voltage of 5.0, the external quantum efficiency is 6.5%.

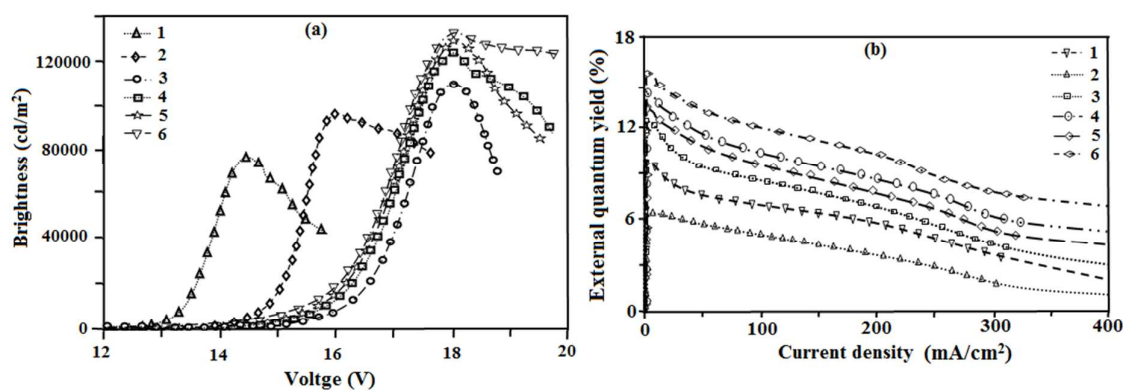


Figure 7. (a) Plot of brightness Vs voltage; (b) Plot of external quantum yield Vs current density

Table 3. Performances of electroluminescence devices I - VI

Device	V _d (V)	L _{max} (cd/m ²)	η _{ext} (%)	η _c (cd/A)	η _p (lm/W)	EL _{max} (nm)
I	3.2	78624, 14.5 V	9.8, 6 V	33.9, 6 V	23.2, 5.0 V	563
II	5.0	98214, 16 V	6.5, 9.5 V	22.2, 9.5 V	9.4, 9.5 V	578
III	3.5	110421, 18 V	12.8, 8 V	42.1, 8 V	24.0, 7 V	572
IV	3.0	124568, 18 V	14.0, 8 V	47.5, 8 V	25.6, 7 V	584
V	3.5	128301, 18 V	13.1, 8 V	44.6, 8 V	26.0, 7 V	561
VI	3.0	131923, 18 V	15.6, 8 V	49.9, 8 V	27.2, 7 V	564

V_d: Driving voltage; L_{max}: Luminous efficiency; η_c: Current efficiency; EL_{max}: Electroluminescence maxima; η_p: Power efficiency; η_{ext}: External quantum yield

The efficiency roll-off may be due to triplet-triplet annihilation [TTA - $3M^* + 3N^* \rightarrow 1M + 3N^*$] and triplet-polaron annihilation [TPA - $3M^* + N^- \rightarrow 1M + N^{-*}$] as reported in the literature [69]. Baldo *et al.*, [70] reported that triplet-triplet annihilation (TTA) is dominant factor for the external quantum efficiency roll-off. Furthermore, Reinke *et al.*, [71] and Aziz *et al.*, [72] advocated that triplet-polaron annihilation (TPA) could be the only source for efficiency roll-off at high current densities. Simple illustration of these processes is shown in figure 8a. Devices III and IV show better performance in terms of brightness of 110421 cd/m^2 and 124568 cd/m^2 at 18 V, respectively. Device IV shows a high power efficiency of 25.6 lm/w at 7.0 V (Figure 8b) and current efficiency (Figure 8c) of 47.5 cd/A at 8.0 V. From the electroluminescent analysis it was concluded that device efficiency was improved by replacing the ancillary ligand from picolinic acid to 4-N,N-dimethylaminopicolinic acid.

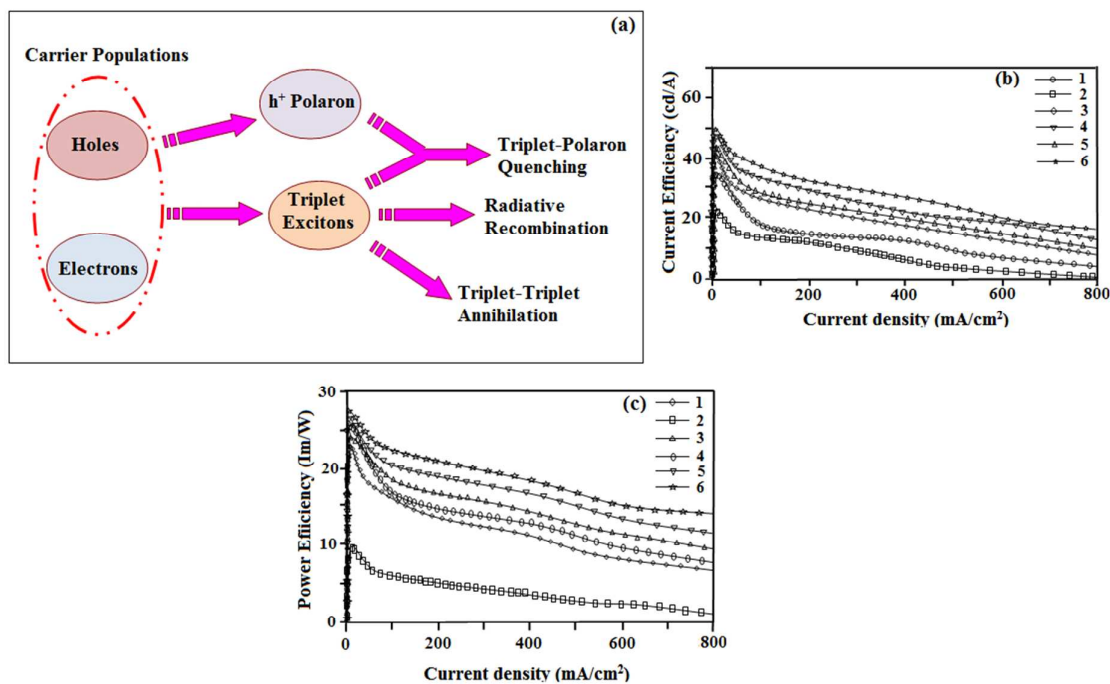


Figure 8. (a) A schematic illustration of TTA and TPA processes; (b) Plot of current efficiency Vs current density; (c) Plot of power efficiency Vs current density

4. Conclusions

We have synthesized a series of iridium complex dopants with appreciable quantum efficiencies, using various substituted bulky phenanthrimidazole ligands. The phosphorescence of these complexes is attributed to a mixture of $^3\text{MLCT}$ and $^3\pi\text{-}\pi^*$. Complexes **1-3**, **5** and **6** display vibronic progressions having excited state with large contribution of $^3\pi\text{-}\pi^*$, whereas the emission spectrum of complex **4** is broad in shape and has excited state with large contribution of $^3\text{MLCT}$. The devices exhibit maximum external quantum efficiency and maximum power and current efficiencies. Devices with dopants $\text{Ir}(\text{tmpmp})_2(\text{pic})$ and $\text{Ir}(\text{tmpdp})_2(\text{pic})$ show better performance in terms of brightness of 110421 cd/m^2 and 124568 cd/m^2 at 18 V, respectively. Device with complex $\text{Ir}(\text{tmpdp})_2(\text{pic})$ shows a high power efficiency of 25.6 lm/w at 7.0 V and current efficiency of 47.5 cd/A at 8.0 V. Device efficiency was improved by replacing the ancillary ligand from picolinic acid to 4-N,N-dimethylaminopicolinic acid.

5. Acknowledgements

One of the authors Prof. J. Jayabharathi is thankful to DST [No. SR/S1/IC-73/2010], DRDO (NRB-213/MAT/10-11), UGC (F. No. 36-21/2008 (SR)), CSIR (NO 3732/NS-EMRII) and SERB (F.No. EMR/2014/000094) for providing funds to this research study.

References

- [1] C.W. Tang and S.A. Vanslyke, *Appl. Phys. Lett.*, 1987, **51**, 913-915.
- [2] M.A. Baldo, S. Lamansky, P.E. Burrows, M.E. Thompson and S.R. Forrest, *Appl. Phys. Lett.*, 1999, **75**, 4.
- [3] Y. Chi and P.T. Chou, *Chem. Soc. Rev.*, 2007, **36**, 1421-1431.
- [4] Y. Chi and P.T. Chou, *Chem. Soc. Rev.*, 2010, **39**, 638-655.
- [5] G. Zhou, W.Y. Wong and X. Yang, *Chem. Asian J.*, 2011, **6**, 1706-1727.
- [6] P. Wang, S.J. Liu, Z.H. Lin, X.C. Dong, Q. Zhao, W.P. Lin, M.D. Yi, S.H. Ye, C.X. Zhu and W. Huang, *J. Mater. Chem.*, 2012, **22**, 9576- 9588.
- [7] M. Ikai, S. Tokito, Y. Sakamoto, T. Suzuki and Y. Taga, *Appl. Phys. Lett.*, 2001, **79**, 156-158.
- [8] A. Kohler, J.S. Wilson and R.H. Friend, *Adv. Mater.*, 2002, **14**, 701-707.
- [9] A.B. Tamayo, B.D. Alleyne, P.I. Djurovich, S. Lamansky, I. Tsyba, N.N. Ho, R. Bau and M.E. Thompson, *J. Am. Chem. Soc.*, 2003, **125**, 7377-7387.
- [10] L. Xiao, Z. Chen, B. Qu, J. Luo, S. Kong, Q. Gong and J. Kido, *Adv. Mater.*, 2011, **23**, 926-952.
- [11] Q. Zhao, S. Liu, M. Shi, C. Wang, M. Yu, L. Li, F. Li, T. Yi and C. Huang, *Inorg. Chem.*, 2006, **45**, 6152-6160.
- [12] F. Zhang, L. Duan, J. Qiao, G. Dong, L. Wang and Y. Qiu, *Org. Electron.*, 2012, **13**, 1277-1288.
- [13] T. Hu, L. Duan, J. Qiao, L. He, D. Zhang, R. Wang, L. Wang and Y. Qiu, *Org. Electron.*, 2012, **13**, 1948-1955.
- [14] W.J. Xu, S.J. Liu, T.C. Ma, Q. Zhao, A. Pertegás, D. Tordera, H.J. Bolink, S.H. Ye, X.M. Liu, S. Sun and W. Huang, *J. Mater. Chem.*, 2011, **21**, 13999-14007.
- [15] B. Chen, Y. Li, W. Yang, W. Luo and H. Wu, *Org. Electron.*, 2011, **12**, 766-773.

- [16] F. Dumur, G. Nasr, G. Wantz, C.R. Mayer, E. Dumas, A. Guerlin, F. Miomandre, G. Clavier, D. Bertin and D. Gigmes, *Org. Electron.*, 2011, **12**, 1683-1694.
- [17] W.J. Xu, S.J. Liu, X.Y. Zhao, S. Sun, S. Cheng, T.C. Ma, H.B. Sun, Q. Zhao and W. Huang, *Chem. Eur. J.*, 2010, **16**, 7125-7133.
- [18] Q. Zhao, F. Li, S. Liu, M. Yu, Z. Liu, T. Yi and C. Huang, *Inorg. Chem.*, 2008, **47**, 9256-9264.
- [19] C. Yang, X. Zhang, H. You, L. Zhu, L. Chen, L. Zhu, Y. Tao, D. Ma, Z. Shuai and J. Qin, *Adv. Funct. Mater.*, 2007, **17**, 651-661.
- [20] B. Liang, L. Wang, Y.H. Xu, H.H. Shi and Y. Cao, *Adv. Funct. Mater.*, 2007, **17**, 3580-3589.
- [21] X. Gong, M.R. Robinson, J.C. Ostrowski, D. Moses, G.C. Bazan and A. Heeger, *J. Adv. Mater.*, 2002, **14**, 581-585.
- [22] R.N. Bera, N. Cumpstey, P.L. Burn, I.W. Samuel, *Adv. Funct. Mater.*, 2007, **17**, 1149-1152.
- [23] Z.W. Xu, Y. Li, X.M. Ma, X.D. Gao and H. Tian, *Tetrahedron*, 2008, **64**, 1860-1867.
- [24] Z.Y. Xia, X. Xiao, J.H. Sua, C.S. Chang, C.H. Chen, D.L. Li and H. Tian, *Synth. Met.*, 2009, **159**, 1782-1785.
- [25] T. H. Kwon, M.K. Kim, J. Kwon, D.Y. Shin, S.J. Park, C.L. Lee, J.J. Kim and J.I. Hong, *Chem. Mater.*, 2007, **19**, 3673-3680.
- [26] P. Coppo, E.A. Plummer and L. De Cola, *Chem. Commun.*, 2004, **15**, 1774-1775.
- [27] M.A. Baldo, D.F. O'Brien, Y. You, A. Shoustikov, S. Sibley, M.E. Thompson and S.R. Forrest, *Nature*, 1998, **395**, 151-154.
- [28] C.L. Li, Y.J. Su, Y.T. Tao, P.T. Chou, C.H. Chien, C.C. Cheng and R.S. Liu, *Adv. Funct. Mater.*, 2005, **15**, 387-395.
- [29] Y. You and S.Y. Park, *J. Am. Chem. Soc.*, 2005, **125**, 12438-12439.

- [30] L.L. Wu, I.W. Sun and C.H. Yang, *Polyhedron*, 2007, **26**, 2679-2685.
- [31] T. Sajoto, P.I. Djurovich, A. Tamayo, M. Yousufuddin, R. Bau and M.E. Thompson, *Inorg. Chem.*, 2005, **47**, 7992-8003.
- [32] R.S. Lumpkin, E.M. Kober, L.A. Worl, Z. Murtaza and T.J. Meyer, *J. Phys. Chem.*, 1990, **94**, 239-243.
- [33] T. Fei, X. Gu, M. Zhang, C. Wang, M. Hanif, H. Zhang and Y. Ma, *Synth. Met.*, 2009, **159**, 113–118.
- [34] (a) Z. K. Chen, W. Huang, L. H. Wang, E. T. Kang, B. J. Chen, C. S. Lee and S. T. Lee, *Macromolecules*, 2000, **33**, 9015-9025; (b) H. S. Joshi, R. Jamshidi and Y. Tor, *Angew. Chem., Int. Ed.* 1999, **38**, 2722; (c) J. N. Demas and G. A. Crosby, *J. Phys. Chem.*, 1971, **75**, 991; (d) J. Jayabharathi, V. Thanikachalam and K. Saravanan, *J. Photochem. Photobiol. A.*, 2009, **208**, 13-20.
- [35] J. Jayabharathi, V. Thanikachalam, M. Venkatesh Perumal and N. Srinivasan, *Spectrochim. Acta, Part A.*, 2011, **79**, 236-244.
- [36] S. Okada, K. Okinaka, H. Iwawaki, M. Furugori, M. Hashimoto, T. Mukaide, J. Kamatani, S. Igawa, A. Tsuboyama, T. Takiguchi and K. Ueno, *Dalton Trans.*, 2005, **9**, 1583–1590.
- [37] A.D. Becke, *J. Chem. Phys.*, 1993, **98**, 5648-5652.
- [38] Gaussian 03, Revision C.02, M. J. Frisch, G. W. Trucks, H. B. Schlegel, G. E. Scuseria, M. A. Robb, J. R. Cheeseman, J. A. Montgomery, Jr., T. Vreven, K. N. Kudin, J. C. Burant, J. M. Millam, S. S. Iyengar, J. Tomasi, V. Barone, B. Mennucci, M. Cossi, G. Scalmani, N. Rega, G. A. Petersson, H. Nakatsuji, M. Hada, M. Ehara, K. Toyota, R. Fukuda, J. Hasegawa, M. Ishida, T. Nakajima, Y. Honda, O. Kitao, H. Nakai, M. Klene, X. Li, J. E. Knox, H. P. Hratchian, J. B. Cross, V. Bakken, C. Adamo, J. Jaramillo, R. Gomperts, R. E. Stratmann, O. Yazyev, A. J. Austin, R. Cammi, C.

- Pomelli, J. W. Ochterski, P. Y. Ayala, K. Morokuma, G. A. Voth, P. Salvador, J. J. Dannenberg, V. G. Zakrzewski, S. Dapprich, A. D. Daniels, M. C. Strain, O. Farkas, D. K. Malick, A. D. Rabuck, K. Raghavachari, J. B. Foresman, J. V. Ortiz, Q. Cui, A. G. Baboul, S. Clifford, J. Cioslowski, B. B. Stefanov, G. Liu, A. Liashenko, P. Piskorz, I. Komaromi, R. L. Martin, D. J. Fox, T. Keith, M. A. Al-Laham, C. Y. Peng, A. Nanayakkara, M. Challacombe, P. M. W. Gill, B. Johnson, W. Chen, M. W. Wong, C. Gonzalez, and J. A. Pople, Gaussian, Inc., Wallingford CT, 2004.
- [39] M. Nonoyama, *Bull. Chem. Soc. Jpn.*, 1974, **47**, 767-768.
- [40] S. Lamansky, P. Djurovich, D. Murphy, F. Abdel-Razzaq, R. Kwong, I. Tsyba, M. Bortz, B. Mmui, R. Bau and M.E. Thompson, *J. Inorg. Chem.*, 2001, **40**, 1704-1711.
- [41] B.X. Mi, P.F. Wang, M.W. Liu, H.L Kwong, N.B. Wong, C.S. Lee and S.T. Lee, *Chem. Mater.*, 2003, **15**, 3148-3151.
- [42] J. DePriest, G.Y. Zheng, N. Goswami, D.M. Eichhorn, C. Woods and D.P. Rillema, *Inorg. Chem.*, 2000, **39**, 1955-1963.
- [43] E. Baranoff, S. Fantacci, F. D. Angelis, X. Zhang, R. Scopelliti, M. Gratzel and M. K. Nazeeruddin, *Inorg. Chem.*, 2011, **50**, 451-462.
- [44] (a) J. Jayabharathi, V. Thanikachalam, K. Saravanan and N. Srinivasan, *J. Fluoresc.*, 2011, **21**, 65-80; (b) J. Jayabharathi, V. Thanikachalam and R. Sathishkumar, *J. Phys. Org. Chem.*, 2014, **27**, 504-511; (c) J. Jayabharathi, C. Karunakaran, K. Jayamoorthy and P. Vinayagamoorthy, *Mater. Express*, 2014, **4**, 279-292.
- [45] J. Jayabharathi, V. Thanikachalam and K. Jayamoorthy, *J. Organomet. Chem.*, 2014, **761C**, 74-83.
- [46] K. Brooks, Y. Babayan, S. Lamansky, P.I. Djurovich, I. Tsyba, R. Bau and M.E. Thompson, *Inorg. Chem.*, 2002, **41**, 3055-3066.

- [47] J. Jayabharathi, V. Thanikachalam, N. Srinivasan, K. Jayamoorthy and M. Venkatesh Perumal, *J. Fluoresc.*, 2011, **21**, 1813-1823.
- [48] S. Okada, K. Okinaka, H. Iwawaki, M. Furugori, M. Hashimoto, T. Mukaide, J. Kamatani, S. Igawa, A. Tsuboyama, T. Takiguchi and K. Ueno, *Dalton Trans.*, 2005, **9**, 1583–1590.
- [49] A.P. Wilde, K.A. King and R.J. Watts, *J. Phys. Chem.*, 1991, **95**, 629-634.
- [50] M.G. Colombo and H.U. Güdel, *Inorg. Chem.*, 1993, **32**, 3081-3087.
- [51] J. Jayabharathi, V. Thanikachalam and R. Sathishkumar, *J. Fluoresc.*, 2014, **24**, 431-444.
- [52] K.C. Tang, K.L. Liu and I.C. Chen, *Chem. Phys. Lett.*, 2004, **386**, 437-441.
- [53] D.S. McClure, *J. Chem. Phys.*, 1949, **17**, 905-913.
- [54] S.D. Cummings and R. Eisenberg, *J. Am. Chem. Soc.*, 1996, **118**, 1949-1960.
- [55] (a) C. Ulbricht, B. Beyer, C. Friebe, A. Winter and U. S. Schubert, *Adv. Mater.*, 2009, **21**, 4418-4441; (b) R. D. Costa, E. Orti, H. J. Bolink, F. Monti, G. Accorsi and N. Armadori, *Angew. Chem. Int. Ed.*, 2012, **51**, 8178-8211; (c) Y. You and W. Nam, *Chem. Soc. Rev.*, 2012, **41**, 7061-7084.
- [56] (a) F. Alary, M. Boggio-Pasqua, J. L. Heully, C. J. Marsden and P. Vicendo, *Inorg. Chem.*, 2008, **47**, 5259-5266; (b) L. Yang, F. Okuda, K. Kobayashi, K. Nozaki, Y. Tanabe, Y. Ishii and M. A. Haga, *Inorg. Chem.*, 2008, **47**, 7154-7165; (c) E. Jakubikova, R. L. Martin and E. R. Batista, *Inorg. Chem.*, 2010, **49**, 2975-2982.
- [57] (a) D. Escudero, E. Heuser, R. J. Meier, M. Schaferling, W. Thiel and E. Holder, *Chem. Eur. J.*, 2013, **19**, 15639-15644; (b) W. H. Lam, E. S. Lam and V. W. Yam, *J. Am. Chem. Soc.*, 2013, **135**, 15135-15143.
- [58] J.B. Bricks, *Photophysics of Aromatic Molecules*, Wiley-Interscience: London, 1970.

- [59] J. Vicente, A. Arcas, D. Bautista and M.C.R. De Arellano, *J. Organomet. Chem.*, 2002, **663**, 164-172.
- [60](a) G.T. Hwang, H.S. Son, J.K. Ku and B.H. Kim, *J. Am. Chem. Soc.*, 2003, **125**, 11241-11248; (b) M. Kumada and K. Tamao, *Adv. Organomet. Chem.*, 1968, **6**, 19-117. (c) J. Pommerehne, H. Vestweber, W. Guss, R. F. Mahrt, H. Bassler, M. Porsch and J. Daub, *Adv. Mater.*, 1995, **7**, 551-554.
- [61] R. Urban, R. Kramer, S. Mihan, K. Polborn, B. Wagner and W. Beck, *J. Organomet. Chem.*, 1996, **517**, 191-200.
- [62] J. Albert, J.M. Cadena, S. Delgado and J. Granell, *J. Organomet. Chem.*, 2000, **603**, 235-239.
- [63] J. Jayabharathi, V. Thanikachalam, N. Srinivasan and M. Venkatesh Perumal, *J. Fluoresc.*, 2011, **21**, 1585-1597.
- [64] F.I. Wu, H.J. Su, C.F. Shu, L. Luo, W.G. Diao, C.H. Cheng, J.P. Duan and G.H. Lee, *J. Mater. Chem.*, 2005, **15**, 1035-1042.
- [65] I.R. Laskar, S.F. Hsu and T.M. Chen, *Polyhedron*, 2005, **24**, 189-200.
- [66] P.J. Hay, *J. Phys. Chem. A.*, 2002, **106**, 1634-1641.
- [67] F. Neve, A. Crispini, S. Campagna and S. Serroni, *Inorg. Chem.*, 1999, **38**, 2250-2258.
- [68] M.G. Colombo, T.C. Brunold, T. Reidener, H.U. Güdel, M. Förtsch and H.B. Bürgi, *Inorg. Chem.*, 1994, **33**, 545-550.
- [69] (a) Q. Wang, I. W. H. Oswald, M. R. Perez, H. Jia, A. A. Shahub, Q. Qiao, B. E. Gnade and M.A. Omary, *Adv. Funct. Mater.*, 2014, **24**, 4746-4752; (b) Q. Wang, I. W. H. Oswald, M. R. Perez, H. P. Jia, B. E. Gnade and M. A. Omary, *Adv. Funct. Mater.*, 2013, **23**, 5420 -5428; (c) Q. Wang and D. Ma, *Chem. Soc. Rev.*, 2010, **39**, 2387-2398; (d) Q. Wang, J. Ding, D. Ma, Y. Cheng, L. Wang, X. Jing and F. Wang, *Adv. Funct.*

Mater., 2009, **19**, 84-95; (e) B. Q. Wang, J. Ding, D. Ma, Y. Cheng, L. Wang and F. Wang, *Adv. Mater.*, 2009, **21**, 2397-2401.

[70] M. A. Baldo, C. Adachi and S. R. Forrest, *Phys. Rev. B*, 2000, **62**, 10967.

[71] S. Reineke, K. Walzer, and K. Leo, *Phys. Rev., B*, 2007, **75**, 125328.

[72] D. Song, S. Zhao, Y. Luo and H. Aziz, *Appl. Phys. Lett.*, 2010, **97**, 243304.